The electron conduction of photosynthetic protein complexes embedded in a membrane

A. Stamouli[a,b,*], J.W.M. Frenken[b], T.H. Oosterkamp[b], R.J. Cogdell[c], T.J. Aartsma[a]

[a] *Department of Biophysics, Huygens Laboratory, Leiden University, P.O. Box 9504, 2300 RA Leiden, The Netherlands*
[b] *Department of Interface Physics, Kamerlingh Onnes Laboratory, Leiden University, P.O. Box 9504, 2300 RA Leiden, The Netherlands*
[c] *Division of Biochemistry and Molecular Biology, IBLS, University of Glasgow, Glasgow G12 8QQ, UK*

Received 23 November 2003; revised 15 January 2004; accepted 19 January 2004

First published online 30 January 2004

Edited by Peter Brzezinski

Abstract The conductivity of two photosynthetic protein–pigment complexes, a light harvesting 2 complex and a reaction center, was measured with an atomic force microscope capable of performing electrical measurements. Current–voltage measurements were performed on complexes embedded in their natural environment. Embedding the complexes in lipid bilayers made it possible to discuss the different conduction behaviors of the two complexes in light of their atomic structure.

Key words: Atomic force microscopy; Bacterial photosynthesis; Light harvesting 2 complex; Reaction center; Biomolecular electronics

1. Introduction

Photosynthetic organisms use a molecular machinery, the photosynthetic apparatus, to convert solar energy into a useful form of chemical energy. The nano-scale apparatus of photosynthetic organisms has been optimized for low-power output and high-quantum efficiency operation. Advances in X-ray crystallography and optical spectroscopy have provided much insight into the structure and function of the simplest photosynthetic apparatus, that of purple bacteria. The primary reactions of photosynthesis occur by a set of transmembrane protein–pigment complexes called the photosynthetic unit (PSU), which is localized in a system of intracytoplasmic membranes. The PSU consists of light harvesting (LH) complexes and reaction centers (RCs). In particular, in the case of photosynthetic purple bacteria, photons are absorbed by light harvesting 2 (LH2) complexes. The excitation energy is then funneled to the RC where a charge separation takes place followed by electron transport across the membrane. This produces an electrostatic potential and a proton gradient across the membrane, which can be utilized for metabolic processes.

The last years have seen considerable efforts in constructing artificial solar-energy converters either with synthetic molecules where biological functions are mimicked [1] or with biomolecules [2]. An important prerequisite for successfully developing such devices is the ability to correlate the electronic properties to the atomic structure of the molecule. In order to obtain such information one needs to reveal the electronic properties on the single-molecule level. Combining electrical measurements with some form of spatial imaging can do this.

Scanning tunneling spectroscopy is a method to study the surface electronic structure of conductors, semiconductors and molecular absorbates. This method is available in a scanning tunneling microscope (STM), which in addition can directly image the spatial organization of the material. Combined scanning tunneling microscopy and spectroscopy has been used to obtain topographs and current–voltage (*I–V*) characteristics of photosynthetic complexes; plant photosystem II membrane fragments [3–5] and plant photosystem I detergent solubilized RCs [6,7].

Scanning tunneling microscopy on biological samples is complicated due to the low conductivity and heterogeneity of the sample, making the interpretation of the STM topographs difficult and ambiguous. Up to now, there have been no reports of high-resolution imaging of large biological molecules with the STM, contrary to the atomic force microscope (AFM), with which high-resolution imaging of large biological molecules has been demonstrated. In a previous publication [8] we have shown that submolecular resolution of LH2 complexes from a purple bacterium could be obtained with the AFM operating in liquid (Fig. 1A, insert), while molecular resolution was obtained with the AFM operating in ambient conditions. (Sub)molecular resolution was obtained with the use of two-dimensional crystals of reconstituted single photosynthetic complexes in a lipid bilayer (Fig. 1A). The high quality of such samples enables a straightforward interpretation of the AFM images and can be used to begin to define how they make electrical contact with the electrodes.

A field of investigation, in constructing artificial solar-energy converters, has been the orientation of the functional molecules between the two electrodes to define how the molecules and the electrodes make electrical contact. Various methods have been employed to ensure that all molecules lay with their electron transfer pathway axis perpendicular to the electrodes [9]. Devices based on detergent solubilized photosynthetic proteins, for example, make use of chemically modified electrodes to attain significant coverage and to prevent protein denaturation [10].

Using photosynthetic transmembrane proteins embedded in lipid bilayers attached via adsorption on an unmodified substrate does not require any substrate pretreatment, and results

*Corresponding author. Fax: (31)-71-5274451.
E-mail addresses: a.stamouli@chem.leidenuniv.nl (A. Stamouli), frenken@phys.leidenuniv.nl (J.W.M. Frenken), tjerk@phys.leidenuniv.nl (T.H. Oosterkamp), r.cogdell@bio.gla.ac.uk (R.J. Cogdell), aartsma@biophys.leidenuniv.nl (T.J. Aartsma).

0014-5793/04/$30.00
doi:10.1016/S0014-5793(04)00080-8

in stable systems because the proteins are in their native environment.

Here, we report the use of an AFM to obtain topographs in combination with electrical measurements performed on an oriented reconstituted layer of LH complexes and an oriented reconstituted layer of RC in lipid bilayers. Current–voltage measurements were obtained on both complexes. Electrical conductivity relationships of these biological molecules are addressed in terms of their molecular structure.

2. Materials and methods

The experiments were performed using a Multimode IIIa AFM (Veeco, Santa Barbara, CA, USA). A standard STM current-to-voltage converter was used (gain 21×10^6 V/A). Si probes coated with a conductive thin layer of Pt/Ir (EFM) were purchased from Veeco (Santa Barbara, CA, USA). The cantilevers had a nominal spring constant of 2.8 N/m and a typical resonance frequency of 75 kHz.

Supported reconstituted LH2 complexes and RCs in lipid bilayers were produced by detergent removal, using a combination of freeze-thaw and dialysis techniques, starting with detergent solubilized complexes, as described elsewhere [8]. The LH2 complex from *Rhodopseudomonas acidophila* strain 10050 has been successfully resolved with the atomic force microscopy under physiological conditions [8]. It is an oligomer, with an αβ heterodimer as a basic unit [11], Fig. 2A. Each αβ heterodimer binds three bacteriochlorophyll (BChl) molecules and two carotenoid molecules. X-ray crystallography data [11,12] and AFM topographs [8] showed that LH2 consists of nine such subunits. The RC from *Rhodopseudomonas sphaeroides* strain R-26 consists of three protein subunits and cofactors (four molecules of BChla, two molecules of bacteriopheophytin a, one carotenoid, two ubiquinones and one ferrous iron) [13,14], Fig. 2B. The graphical representations of the complexes were made using Protein Explorer (http://www.umass.edu/microbio/chime/explorer/).

Highly ordered pyrolythic graphite (HOPG) (Surface Preparation Laboratory, The Netherlands) was used as a conductive substrate. In the range of voltages used in this study, HOPG does not induce any structure in the *I–V* graphs. The substrates were incubated in the proteo(liposome) solution for 30 min, then rinsed with distilled water and dried under a flow of nitrogen. The samples were imaged immediately afterwards in ambient conditions.

The samples were first imaged with AFM in tapping mode to locate a reconstituted lipid bilayer. When such an area was found, the tapping oscillation of the tip was switched off and the distance between the tip and substrate was decreased until a detectable current was measured. For the *I–V* measurement a linear voltage ramp was applied between the tip and the sample, and the resulting current was measured. On average, 10 *I–V* curves were taken at each location. One of the problems encountered was that the tip quickly got contaminated, due to the roughness of the sample and drifts. Once the curves were no longer reproducible the measurements were stopped and a new probe was utilized. The force exerted by the tip on the biological sample did not exceed 2 nN. This force is probably large enough to cause some deformation, but the overall structure and function of the protein should remain largely intact [15]. This was verified with topographs obtained in tapping mode operation after the acquisition of *I–V* curves. Voltage–force curves showed no significant influence of the applied voltage on the force between the sample and tip. It has been shown previously that the combination of a high spring constant probe and a broad tip apex introduces only weak electrostatic generated forces [17]. The absolute scale of the current measured for both complexes does not correspond to meaningful values, since the current depends strongly on the details of the contact between the probe and the sample, for example on the distance between the conductive probe and the complex, and this distance slightly varied from experiment to experiment.

3. Results and discussion

3.1. Measurements

Fig. 1A shows molecular resolution AFM topographs in ambient conditions of LH2 complexes reconstituted in a lipid bilayer, obtained with an uncoated Si probe. The lateral dimensions of the observed protrusions in the lipid bilayers are ~7.75 nm, which corresponds to single LH2 complexes. Submolecular resolution can be obtained by imaging the reconstituted samples in solution [8]. Fig. 1B shows AFM topographs of the same sample using a Pt/Ir-coated probe. Protrusions are not visible in this topograph since the tip diameter of the coated probe was likely to be broader than ~13 nm (the distance between two neighboring LH2s), resulting in a lower resolution. Topographs of similar quality were obtained with reconstituted RC complexes in lipid bilayers.

Current–voltage measurements were performed on patches as those shown in Fig. 1. Fig. 3 shows the measured current as

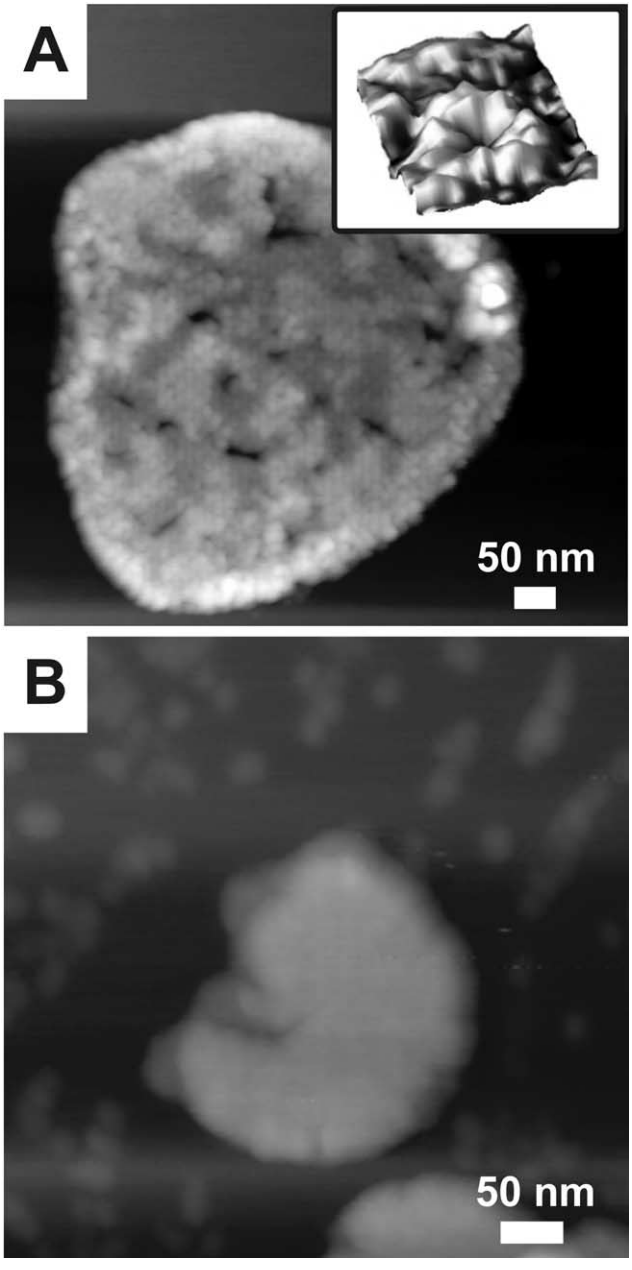

Fig. 1. Molecular resolution AFM topographs of the LH2 complex in lipid bilayers. A: Obtained with a Si tip. Insert: High resolution of a LH2 complex. B: Obtained with a Pt/Ir-coated tip. The gray scales represent height ranges of 20 and 35 nm, respectively.

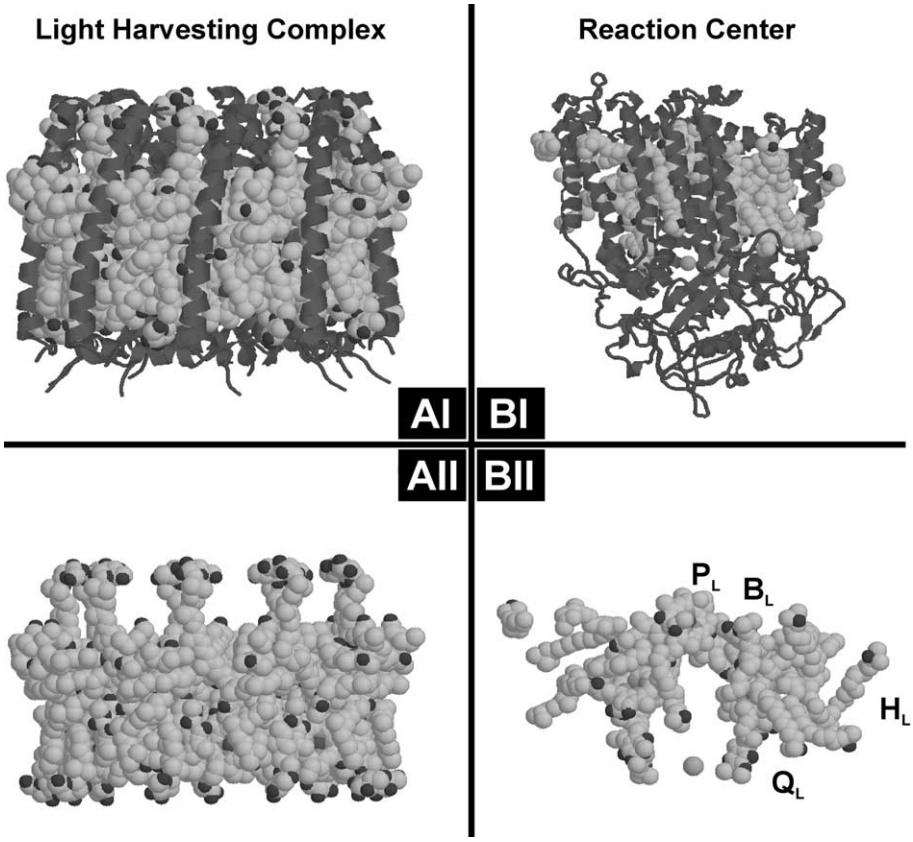

Fig. 2. Atomic structures of the two photosynthetic complexes (top view, periplasmic side). A: The LH2 complex showing (AI) proteins and pigments, and (AII) only the pigment molecules, carotenoids, C, the BChls of the 850 band, B850, the BChls of the 800 band, B800. B: Atomic structure of the RC showing (BI) proteins and pigments, and (BII) only pigments, BChl dimer, P, BChl, B_L, bacteriopheophytin, H_L, and quinone, Q_L are indicated.

a function of the applied voltage between the substrate and tip, for LH2 complexes (Fig. 3A) and for the RCs (Fig. 3B). The adsorbed proteins displayed different *I–V* characteristics. While the *I–V* curves of the LH2 complex were symmetric at about $V = 0$, the *I–V* curves of the RCs were highly asymmetric.

The measured current–voltage curves on reconstituted LH2 and RC protein complexes in lipid bilayers sandwiched be-

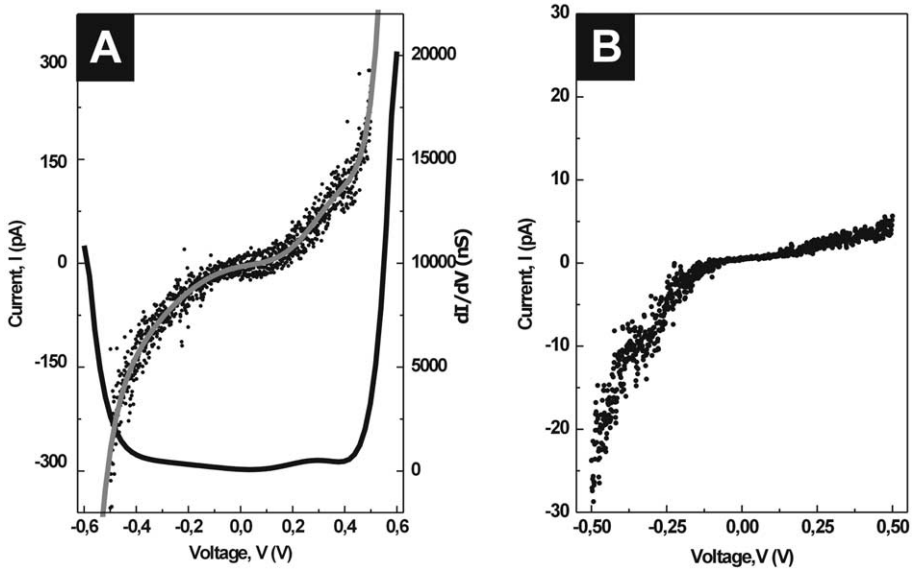

Fig. 3. Current versus voltage curves on oriented protein bilayers, obtained with a bias voltage of ±0.5 V. A: LH2 complex reconstituted sample. The gray line through the points is a polynomial fit to the data. The black line is a differentiate of the polynomial fit. B: RC reconstituted sample.

tween two electrodes show that in these proteins indeed electron transfer takes place. There are various models to account for electron transfer in organic systems, which we will now consider. Firstly, direct tunneling from one electrode (tip) to the other electrode (HOPG substrate). This source of charge propagation can be simply ruled out due to the excessively large tunneling distances [17] that would be involved, 5.6 nm for the LH2 and 7.3 nm for the RC complex. The alternative type of electron transfer is via electronic states existing in the molecule, which could be localized or delocalized over the entire molecule. Since the atomic structures of both proteins have been resolved with X-rays we can attempt to assign a molecular electron transfer pathway for each of them.

3.2. Electron transfer through LH2 complexes

The LH2 protein complex consists of chlorophylls, carotenoids and proteins. The geometrical arrangement of these molecules is shown in Fig. 2AI. The use of oriented samples between the two electrodes makes it possible to exclude several possible electron transfer pathways, as will be discussed below.

Electron transfer could take place between the chlorophylls via tunneling [18]. The chlorophylls in LH2 are arranged in two optically absorbing bands, the so-called 850 (or B850) and 800 (or B800) bands. The 850 nm absorbing chlorophylls are arranged perpendicular to the membrane plane in a ring and lie closest to the periplasmic face of the complex, at a distance of $\sim$0.8 nm. The 800 nm absorbing chlorophylls are arranged with their molecular planes parallel to that of the membrane and lay at $\sim$2.2 nm from the cytoplasmic face of the complex. Also here, the proposed electron transfer scenario that involves electrons tunneling from the B800 chlorophylls to the electrode can be excluded due to the large distance between the B800 chlorophylls and the electrode. The maximum distance reported for electrons traveling through a protein medium is 1.4 nm [17]. The distance between the two chlorophyll rings in the LH2 complex, 2.2 nm, is larger than the 1.4 nm reported tunneling distance, and therefore could not account for the significant measured currents.

More plausible is electron transfer through the carotenoid (rhodopsin-glucoside) molecules. Nine carotenoids are located between the proteins and span the membrane (Fig. 2AI), one carotenoid per αβ heterodimer unit [11]. Recent electron density maps with a higher resolution have revealed a second carotenoid molecule per unit [12]. This second carotenoid lies on the outside of the complex between the β-peptides and is bent. Since it is not clear whether this bend is an in vivo conformation or that it originates from the sample preparation procedure, we will base our discussion on the atomic structure obtained by McDermont et al. [11], i.e. the one without the extra carotenoid.

In photosynthesis carotenoids are essential, they are efficient quenchers of the excited triplet state, thus preventing the formation of singlet oxygen. Carotenoids are conjugated chains, having a backbone of alternating single and double bonds. Electron conduction in polymeric opto-electronic devices has been attributed to the conjugated character of such polymer chains [19]. The presence of alternating single and double bonds is what makes conjugated chains efficient charge carriers: the mutual overlap of the π-orbitals of neighboring atoms, arising from unpaired electrons in the chain, causes the wave functions to delocalize over the whole chain.

Electrical measurements on synthetic β-carotene molecules have been performed by Rosenberg [20] on glass and on crystalline samples, and by Leatherman et al. [16] on oriented samples. The latter measurements have been performed with a conductive AFM on carotenes embedded in an insulating alkanethiol matrix, and revealed symmetric I–V curves around $V=0$. Although the data of [16] did not allow to distinguish between an ohmic or a semiconductor behavior, the resistivity was found to be on the order of 4.2 GΩ per carotenoid. The differential resistivity for carotenoids, outside the gap region, in this study was found to be 1.7 GΩ. We do not know how many carotenoids our tip may be contacting at one time. Also the contact resistance depends on the precise contact geometry and chemistry [21]. The activation energy for semiconductor conductivity of carotenoids as glass and crystalline samples has been measured as 1.5 and 0.8 eV, respectively. These values agree well with the energy gap of carotenoids embedded in lipid bilayers estimated in this study to be larger than 1 eV (Fig. 3A). The presence of oxygen [22] or conformational thermal fluctuations leading to conformational changes [23] may be factors responsible for the absence of very sharp I–V curves. Even so, the values for the resistivity and energy gap are in good agreement with the values measured for carotenoids not embedded in proteins.

Considering all possible scenarios and the similarity between I–V characteristics between single oriented carotene molecules and oriented LH2 complexes, we believe that charge transfer from the tip to the substrate and vice versa takes place via electron injection and conduction through the carotenoid molecules.

3.3. Electron transfer through RC complexes

I–V graphs on films of oriented RCs showed an asymmetry in the conductance between positive and negative bias voltages, in contrast to the symmetric I–V graphs measured for the LH2 complex. The current increases in reverse bias, and remains small in forward bias. Current rectification by organic molecules has been reported in literature for zwitterionic molecules [24], phythalocyanine molecules [25] and photosynthetic RCs from plants [7]. In the case of the photosystem I from plants [7] the current-rectifying I–V curve, obtained with STM, has been attributed to the orientation of the PSI on the surface and has been used to propose in which orientation the molecule preferentially adsorbs on the surface.

In nature, electron transfer indeed takes place in photosynthetic RCs. In Fig. 2BII the atomic structure and molecular electron transfer pathway derived from spectroscopic experiments are depicted. The cofactors, a BChl dimer (P), a BChl molecule (B_L), bacteriopheophytin (H_L) and a quinone (Q_L), are the necessary electron transfer components. Excitation with light or resonance energy transfer from an antenna complex first promotes the electron donor (P) to an excited singlet state. Electrons are then successively transferred from P to B_L (0.47 nm transfer distance), then to H_L (0.38 nm transfer distance) and finally to Q_L (0.9 nm transfer distance).

In this study electrons are injected to P via the AFM tip. We propose that the subsequent electron pathway mentioned above is the same pathway used for electrons in this study. The rate constants for electron transfer in the case of *R. sphaeroides* have been determined. The rates for back electron transfer (Q_L to H_L to B_L to P) are significantly lower than the forward ones [26]. We propose that this difference lies at the

root of the observed asymmetry in the current between positive and negative voltages.

Only asymmetric *I–V* curves displaying higher currents for negative voltages were measured, corresponding to RCs with their cytoplasmic side facing the substrate. The observed orientation unidirectionality of RCs in the lipid bilayer has to do with the mechanism of the reconstitution protocol. For reconstitution of detergent solubilized transmembrane proteins in preformed liposomes, the protein preferentially inserts in the lipid bilayer with its more hydrophobic moiety first (for RCs, the periplasmic side is the most hydrophobic, as revealed from the X-ray structure), thus exposing its more hydrophilic part to the exterior of the lipid bilayer. With rupture of the proteoliposomes on the substrate the interior of the proteoliposome (which is the periplasmic side) is exposed to the AFM tip [8].

The RC is thus attached to the substrate via the hydrophilic protein subunit H. The largest part of this unit extends outside of the lipid bilayer, by about 3 nm. It is a low-density protein and can therefore change its conformation or easily gets deformed to the extent that electrons can reach the electrode, substrate. We cannot rule out that the observed asymmetry in the measured *I–V* curves is due to the formation of a Schottky barrier. Schottky barriers are formed when a metal is brought in physical contact with a semiconductor; at the interface, the Fermi level of the semiconductor is pinned by defect or interface states and the overall electrical properties of the device are dominated by the resulting Schottky barrier height. However, the observation that we invariably find the same *I–V* behavior on many different locations on the RC films, obviously with different contact geometries of the tip and substrate sites suggests that the rectifying behavior is an intrinsic property of the RC complex.

Before the acquisition of every *I–V* curve the distance between the tip and material in our setup was reduced so as to measure a detectable current. Further decreasing the distance between the tip and sample with LH2 complexes did not result in asymmetric *I–V* curves. Possible effects of material/protein deformation could be pursued further by performing experiments through electrical contacts consisting of small gold particles covalently bound to the protein [27]. However, this would require protein engineering to introduce cysteines at selected sites.

One of the open questions in photosynthesis is the spatial organization of the photosynthetic apparatus. Clearly, optimal performance of the LH and RC complexes can be expected only if these occupy strategic positions with respect to each other. Using AFM topographs, it may be quite difficult to answer this question. Special sample preparation methods and high-resolution AFM imaging have to be employed, since the dimensions of these complexes are very similar [28]. However, if the topographic resolution obtained with conductive probes can be improved, electrical measurements, as shown here, in combination with AFM topographs can possibly be used as an easier route to identify the different complexes in photosynthetic membranes and in this way directly image the organization of the photosynthetic apparatus by a conductivity map.

4. Conclusions

Using an AFM capable of performing electrical measurements we have measured the electrical conduction properties of two photosynthetic protein complexes, a LH complex and a RC. The conduction was measured as a function of applied voltage. Whereas the LH complex exhibited a symmetric current–voltage behavior, the RC exhibited a pronounced asymmetry. Using the atomic structures of these complexes, known from X-ray crystallography, and their well-defined orientation in lipid bilayer samples we were able to suggest a plausible electron pathway for each of the two complexes. We propose that the electron conduction of LH2 complexes takes place through the carotenoid molecules, which span the gap and can be seen as molecular wires. The measured conduction in this system was in good agreement with conduction measurements of isolated oriented carotenoids. We propose that electron transfer through the RC occurs through the cofactors. The asymmetric current–voltage curves for the RCs are attributed to the difference between the forward and back transfer rates, known for this cofactor combination.

Acknowledgements: The authors would like to thank Jim Flach of Veeco Instruments for the modifications of the Nanoscope software necessary for the experiments, and Martien van de Pijl and Martin Moene from the University Leiden for hardware and software aid. This work is part of the research program of the Stichting voor Fundamenteel Onderzoek der Materie (FOM) and was made possible by financial support from the Nederlandse Organisatie voor Wetenschappelijk Onderzoek (NWO). R.J.C. was funded by the BBSRC agency.

References

[1] Cogdell, R.J. and Lindsay, J.G. (1998) Trends Biotechnol. 16, 521–527.
[2] Fujihira, M., Sakomura, M., Aoki, D. and Koike, A. (1996) Thin Solid Films 273, 168–176.
[3] Lukins, P.B. (1999) Biochem. Biophys. Res. Commun. 256, 288–292.
[4] Lukins, P.B. and Oates, T. (1998) BBA Bioenerg. 1409, 1–11.
[5] Lukins, P.B. (2000) Chem. Phys. Lett. 321, 13–20.
[6] Lee, I., Lee, J.W., Warmack, R.J., Allison, D.P. and Greenbaum, E. (1995) Proc. Natl. Acad. Sci. USA 92, 1965–1969.
[7] Lee, I., Lee, J.W. and Greenbaum, E. (1997) Phys. Rev. Lett. 79, 3294–3297.
[8] Stamouli, A., Kafi, S., Klein, D.C.G., Oosterkamp, T.H., Frenken, J.W.M., Cogdell, R.J. and Aartsma, T.J. (2003) Biophys. J. 84, 2483–2491.
[9] Imahori, H., Mori, Y. and Matano, Y. (2003) J. Photochem. Photobiol. C Photochem. Rev. 4, 51–83.
[10] Ogawa, M., Kanda, R., Dewa, T., Iida, K. and Nango, M. (2002) Chem. Lett. 4, 466–467.
[11] McDermott, G., Prince, S.M., Freer, A.A., Hawthornwaite-Lawless, A.M., Paziz, M.Z., Cogdell, R.J. and Isaacs, N.W. (1995) Nature 374, 517–521.
[12] Papiz, M.Z., Prince, S.M., Howard, T., Cogdell, R.J. and Isaacs, N.W. (2003) J. Mol. Biol. 326, 1523–1538.
[13] Allen, J.P., Feher, G., Yeates, T.O., Komiya, H. and Rees, D.C. (1987) Proc. Natl. Acad. Sci. USA 84, 6162–6166.
[14] Allen, J.P., Feher, G., Yeates, T.O., Komiya, H. and Rees, D.C. (1987) Proc. Natl. Acad. Sci. USA 84, 5730–5734.
[15] Andreas, E., Lyubchenko, Y. and Müller, D.J. (1999) Trends Cell Biol. 9, 77–80.
[16] Leatherman, G., Durantini, E.N., Gust, D., Moore, T.A., Moore, A.L., Stone, S., Zhou, Z., Rez, P., Liu, Y.Z. and Lindsay, S.M. (1999) J. Phys. Chem. B 103, 4006–4010.
[17] Page, C.C., Chen, X., Moser, C.C. and Dutton, P.L. (1999) Nature 402, 47–52.
[18] Nelson, R.C. (1957) J. Chem. Phys. 27, 864–867.
[19] Shirakawa, H., Louis, E.J., MacDiarmid, A.G., Chiang, C.K. and Heeger, A.J. (1977) J. C. S. Chem. Commun. 578–580.
[20] Rosenberg, B. (1959) J. Chem. Phys. 31, 238–245.

[21] Di Ventra, M., Pantelides, S.T. and Lang, N.D. (2000) Phys. Rev. Lett. 84, 979–982.
[22] Rosenber, B. (1961) J. Chem. Phys. 34, 812–819.
[23] Grüner, G. (1994) Density Waves in Solids, Addison-Wesley Publishing Co., Reading, MA.
[24] Martin, A.S., Sambles, J.R. and Ashwell, G. (1993) Phys. Rev. Lett. 70, 218–221.
[25] Pomerantz, M., Aviram, A., McCorkle, R.A., Li, L. and Schrott, A.G. (1992) Science 255, 1115–1118.
[26] Shinkarev, V.P. and Wraigt, C.A. (1993) in: The Photosynthetic Reaction Center (Deisenhofer, J. and Norris, J.R., Eds.), Vol. 11, pp. 193–255, Academic Press, New York.
[27] Cui, X.D., Primak, A., Zarate, X., Tomfohr, J., Sankey, O.F., Moore, A.L., Moore, T.A., Gust, D., Harris, G. and Lindsay, S.M. (2001) Science 294, 571–574.
[28] Scheuring, S., Seguin, J., Marco, S., Levy, D., Robert, B. and Rigaud, J.L. (2003) Proc. Natl. Acad. Sci. USA 100, 1690–1693.